Precise predictions of stellar occultations by Pluto, Charon, Nix and Hydra for 2008-2015[,⋆,⋆⋆,⋆⋆⋆,†]

M. Assafin[1], J. I. B. Camargo[2,1], R. Vieira Martins[2,1,‡], A. H. Andrei[2,1,§], B. Sicardy[4,5], L. Young[6], D. N. da Silva Neto[3,1], F. Braga-Ribas[2,1]

[1] Observatório do Valongo/UFRJ, Ladeira Pedro Antonio 43, CEP 20.080-090 Rio de Janeiro - RJ, Brazil
  e-mail: `massaf@astro.ufrj.br`
[2] Observatório Nacional/MCT, R. General José Cristino 77, CEP 20921-400 Rio de Janeiro - RJ, Brazil
  e-mail: `rvm@on.br`
[3] Centro Universitário Estadual da Zona Oeste, Av. Manual Caldeira de Alvarenga 1203, CEP: 23.070-200 Rio de Janeiro - RJ, Brazil
  e-mail: `darionneto@gmail.com`
[4] Observatoire de Paris/LESIA, Meudon, France
  e-mail: `bruno.sicardy@obspm.fr`
[5] Université Pierre et Marie Curie, Institut Universitaire de France, Paris, France
  e-mail: `bruno.sicardy@obspm.fr`
[6] Southwest Research Institute, 1050 Walnut St, Boulder, CO 80302
  e-mail: `layoung@boulder.swri.edu`

ABSTRACT

Context. Investigation of transneptunian objects, including Pluto and its satellites, by stellar occultations.

Aims. Derive precise, astrometric predictions for stellar occultations by Pluto and its satellites Charon, Hydra and Nix for 2008–2015. Construct an astrometric star catalog in the UCAC2 system covering Pluto′s sky path.

Methods. We have carried out in 2007 an observational program at the ESO2p2/WFI instrument covering the sky path of Pluto from 2008 to 2015. Astrometry of 110 GB of images was made by using the Platform for Reduction of Astronomical Images Automatically (PRAIA). By relatively simple astrometric techniques, we have treated the overlapping observations and derived a Field Distortion Pattern for the WFI mosaic of CCDs to within 50 mas precision.

Results. Positions were obtained in the UCAC2 frame with errors of 50 mas for stars up to magnitude R = 19, and 25 mas up to R = 17. New stellar proper motions were also determined using 2MASS and USNO B1.0 catalog positions as first epoch. We have generated 2252 predictions of stellar occultations by Pluto, Charon, Hydra and Nix for 2008–2015. An astrometric catalog with proper motions was produced, containing 2.24 million stars covering Pluto′s sky path with 30′ width. Its magnitude completeness is about R = 18–19 with limit about R = 21. Based on past 2005–2008 occultations successfully predicted, recorded and fitted, a linear drift with time in declination with regard to DE418/plu017 ephemerides was determined for Pluto and used in the current predictions. For *offset (mas)* = $A * (t(yr) - 2005.0) + B$, we find A = +30.5 ±4.3 mas yr^{-1} and B = −31.5 ±11.3 mas, with standard deviation of 14.4 mas for the offsets. For these past occultations, prediction and follow up observations were made with the 0.6m and 1.6m telescopes at the Laboratório Nacional de Astrofísica/Brazil.

Conclusions. Here, recurrent issues in stellar occultation predictions were addressed and properly overcome: body ephemeris offsets, catalog zero-point position errors and Field-of-View size, long term predictions and stellar proper motions, faint-visual versus bright-infrared stars, star/body astrometric follow up. In particular, we highlight the usefulness of the obtained astrometric catalog as a reference frame for star/body astrometric follow up before and after future events involving the Pluto system. Besides, it also furnishes useful photometric information for field stars in the flux calibration of observed light curves. Updates on the ephemeris offsets and candidate star positions (geometric conditions of predictions and finding charts) are made available in a continuous basis by the group at http://www.lesia.obspm.fr/perso/bruno-sicardy/.

Key words. Astrometry – Occultations – Planets and satellites: individual: Pluto, Charon, Nix, Hydra

1. Introduction

Investigating physical properties of Pluto and its satellites is essential for understanding transneptunian objects, keystones in the study of structure, origin and evolution of the Solar System.

Lower/upper limits of 1,169–1,172 km and 1,190-1,193 km for Pluto's radius are given by the combination of gaseous CH_4 spectra and stellar occultation observations (Lellouch et al. 2009). Charon radius ranges from 603.6 ±1.4 km to 606.0 ±1.5 km, as estimated by various authors from the 11 July 2005 stellar occultation (Sicardy et al. 2006; Gulbis et al. 2006; Person et al. 2006). GM values of 870.3 ± 3.7, 101.4 ± 2.8, 0.039 ± 0.034 and 0.021 ± 0.042 $km^3 \ s^{-2}$ are estimated respectively for Pluto, Charon, Nix, and Hydra (Tholen et al. 2008). This results in densities of 1.8–2.1 $g \ cm^{-3}$ and 1.55–1.80 $g \ cm^{-3}$ for Pluto and Charon, with rock versus ice fractions of 0.65 and of 0.55-0.60, respectively, in agreement with current structural models (McKinnon et al. 1997). Nix and Hydra estimated diameters are 88 km and 72 km, assuming a density of 1.63 gm cm^{-3} like Charon (Tholen et al. 2008).

Stellar occultations have unveiled surprising features in Pluto's tenuous μbar-level atmosphere. Its upper atmosphere is isothermal with T $\approx$ 100 K above about 1215 km from the center. Pressure roughly doubled between 1988–2002 after Pluto's 1989 perihelion passage and then has stabilized over 2002-2007 (Sicardy et al. 2003; Elliot et al. 2003; Elliot et al. 2007; Young et al. 2008). Pluto's atmosphere is about 99.5 % N_2, 0.5 % ± 0.1 % CH_4 and some undetermined amount of CO (Lellouch et al. 2009). The molecular nitrogen is in vapor-pressure equilibrium with the N_2 frost at the surface. Even so, the tiny amount of methane is known to be able to produce a pronounced thermal inversion layer. Indeed, about 10 km below 1215 km, there is a remarkable thermal inversion which is probably caused by methane heating (see Yelle & Lunine 1989 and Lellouch et al. 2009 for details).

The 2005 stellar occultation by Charon brought stringent constraints on the presence of an atmosphere. Considering a surface temperature of 56 K rising up to 100 K above 20 km, a pure N_2 or CH_4 isothermal atmosphere leads to pressure limits respectively of 15 μbar and 110 μbar (Sicardy et al. 2006). These low values are compatible with the expected volatile scape rates for Charon (Yelle & Elliot 1997).

In spite of all this knowledge, Pluto's radius is still dependent on atmospheric models (Stansberry at al. 1994; Lellouch et al. 2009). Also, the thermal inversion could alternatively be explained by the presence of a thin haze layer with opacity >0.15 in vertical viewing. Moreover, because the N_2 vapor pressure is a steep function of temperature, an instantaneous response of the surface to insolation decay of about 3 % should have led to a pressure decrease by a factor of 1.4 between 1988 and 2002, instead of the observed increase by a factor of about two. All this points to more complex scenarii at work over the 248-year Pluto's orbital period. Seasonal effects associated with the recent passage through its equinox (December 1987), also at perihelion epoch (September 1989), may have led to the redistribution of ices on Pluto's surface. For instance, the recently sunlit southern cap could now sublimate its nitrogen ice, thus feeding the atmosphere with more N_2 in spite of the decreasing solar energy available. A time lag is now necessary for this nitrogen to condense near the now permanently non-illuminated northern polar region. This kind of scenarii was actually foreseen in the work by Hansen & Paige (1996). Their best model predicted a pressure maximum in 2005 and a significant decrease only after 2025. Pressure would only be restored back to the 1988 levels in the 2100's. These models are not unique, however, and although they capture the basic physics behind those large pressure variations, the amplitude and duration of the present surge may have significant discrepancy when compared to models.

Note also that any re-evaluation of Charon's radius implies a change on its density estimates and ultimately in the ice/silicate ratio. Moreover, any stellar occultation by Nix or Hydra will become a benchmark for the Pluto-Charon system. Size and shape could be obtained at kilometer-level precision, finally leading to the determination of density and ice/rock ratio for these small satellites. This in turn would allow for a better selection among plausible scenarios for the collisional history of the Pluto system. The same could be said of serendipitous detection of orbiting material.

All this strongly supports observation of stellar occultations by Pluto and its satellites. In the forthcoming years, there will be no other observational alternative available to probing at high spatial resolution (km accuracy) Pluto's atmospheric structure between the surface and about 150 km altitude, at least until 2015 when the New Horizons Space Mission probe arrives at Pluto. In this context, efforts toward new and precise predictions for future occultations are important. Note that until the 2000's, the Pluto-Charon system has been only probed almost exclusively by the 1988 mutual events between Pluto and Charon. Furthermore, a stellar occultation observed in 1985 revealed Pluto's atmosphere (Brosch 1995), which was observed more extensively during another occultation in 1988 (Millis et al. 1993). Also, besides the first stellar occultation recorded for Charon (Walker 1980), only two others have been so far observed (11 July 2005 and 22 June 2008).

The first consistent efforts for prediction of stellar occultations by Pluto are described in Mink & Klemola (1985) and cover the period 1985–1990. After that, it is only worth noting the work by McDonald & Elliot (2000a, 2000b), now covering the period 1999–2009. Two important common limitations were the astrometric precision of about only 0″2 and the lack of stellar proper motions leading to uncertainties of the order of the Earth radius for the predicted shadow paths. Also, these earlier predictions were degraded by poorer precision of older ephemerides, an issue which has been changing with the constant feed of new Pluto positions.

To overcome these and other problems, we have carried out an observational program at the ESO2p2/WFI instrument during 2007 and derived precise positions for determining accurate predictions of stellar occultations by Pluto and its satellites Charon, Nix and Hydra for the period 2008–2015.

In Sect. 2, we further develop the astrometric context of predictions and the rationale of the ESO2p2/WFI program. In Section 3 we describe the observations. The astrometric treatment is detailed in Sect. 4. As an important part of the work, the derived catalog of star positions along Pluto's sky path is presented in Sect. 5. Next, in Sect. 6, we describe the

determination of ephemeris offsets for Pluto - a necessary refinement for the predictions. The candidate star search procedure is explained in Sect. 7. Predictions of stellar occultations by Pluto and its satellites are finally presented in Sect. 8 and results are discussed in Sect. 9.

2. Stellar occultation predictions: astrometric rationale

Following the release of the ICRS (Arias et al. 1995; Feissel & Mignard 1998) and of the HIPPARCOS catalog (Perryman et al. 1997), denser and astrometrically more precise catalogs became available in the 2000's, such as the UCAC2 (Zacharias et al. 2004), the 2MASS (Cutri et al. 2003), the USNO B1.0 (Monet et al. 2003) and the GSC2.3 (Lasker et al. 2008). Not by chance, a remarkable improvement in the prediction of stellar occultations has taken place since then. Telescopes equipped with CCDs with relatively small FOV (Field-of-View) could now be used. Not only provisional positions of candidate stars could thus be improved, but also better estimates for the Pluto ephemeris offsets could also be derived. Another factor was the entering of Pluto in front of the projected Galactic plane, increasing the frequency of possible events. Successful examples of such new prediction methods are the stellar occultation campaigns of 2002 (Pluto) and 2005 (Charon).

Since 2004, our group has been engaged on a systematic effort to derive astrometric predictions for stellar occultations by Pluto and its satellites. Using meter-class telescopes and refined astrometric methods, precise positions based in the UCAC2 catalog have been obtained since then, not only for candidate stars but also for Pluto itself. A number of stellar occultations between 2005–2008 have been foreseen and successfully observed as predicted for stars between $13 < R < 16$. Synthetic light curves have been fitted to those observations, providing among other results, Pluto's offset relative to its ephemeris, and revealing a clear linear drift in time for declination. This drift can yield to declination offsets larger than 100 milli-arcseconds (mas) for 2009 (see Sect. 6). This is comparable to Pluto's apparent angular diameter. By knowing the ephemeris offset, we could foresee events for Pluto up to 2015. Since the orbits of Charon, Nix and Hydra around Pluto are well known, we could also extend stellar occultation predictions to these satellites.

As time goes by, mostly for magnitudes fainter than about $R = 14$, estimation of star coordinates for current and future events is severely degraded by increasing errors in proper motion and mean catalog position, amounting to budget uncertainties of more than 70 mas in the UCAC2 case. Position errors can be even worse than 100–200 mas in the case of 2MASS, USNO B1.0 and GSC2.3 catalogs. In this magnitude regime, predictions based solely on such catalog positions start to become unusable. This is important, as fainter - thus, more numerous - objects are becoming more and more accessible to modern detectors.

Moreover, as Pluto passes in front of regions of denser molecular clouds in the Galactic plane, chances are that relatively faint V or R, but bright infrared-emitting stars might be missed. Another issue is the problem of zero-point reference frame errors inherent to small FOV astrometry.

To overcome these problems, an observational program was carried out at the ESO2p/WFI instrument during 2007. Precise positions were obtained and accurate predictions derived for stellar occultations by Pluto and its satellites Charon, Nix and Hydra. The astrometry of about 110 GB of acquired/processed images was accomplished with the Platform for Reduction of Astronomical Images Automatically - PRAIA (Assafin 2006). The software provides astrometric solutions suitable for the overlapping WFI CCD moscaics. The covered sky path of Pluto extended from 2008 to 2015 - year of the New Horizons probe close encounter with the system. Results for 2008 and 2009 were also included because they might be eventually useful for the adjustment of occultations not yet published and for external checks of the accuracy of our predictions. In the astrometry, we have derived a Field Distortion Pattern for the WFI mosaic of CCDs within 50 mas precision. Another feature of our astrometric procedure was the determination of star proper motions using the 2MASS and USNO B1.0 catalogs as first epoch. In this way, we have minimized position error propagation to the 2015 predictions.
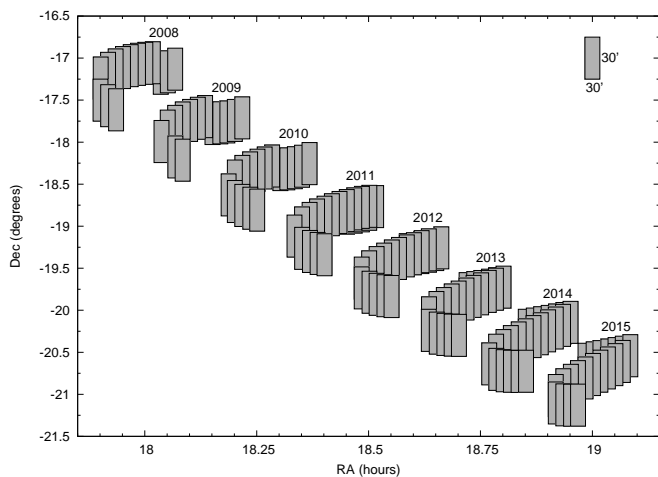
From the above procedures, an astrometric catalog of $30'$ width was derived encompassing the 2008–2015 sky path of Pluto. It is in the UCAC2 reference frame with magnitude completeness around $R = 18$–19 and limiting magnitude about $R = 21$. Having about 2.24 million stars and available in electronic form, the catalog can be very useful in the astrometric calibration of small CCD fields around Pluto and candidate stars, for refining occultation predictions and for star/body astrometric follow up before and after event date. It can be also helpful for deriving the photometric properties of flux calibration stars in the occultation FOV.

As mentioned before, to improve the accuracy of current predictions for occultations up to 2015, precise ephemeris offsets were derived, based on an independent set of precise star positions and on fittings to previous Pluto and Charon stellar occultations observed during 2005–2008 in past campaigns. The predictions of those past events were updated by an astrometric follow-up program carried out in that period at the B&C 0.6 m telescope of the Laboratório Nacional de Astrofísica (LNA), Brazil. From this follow-up program comes the aforementioned independent set of precise star positions (see more details in Sect. 6).

For the future events here predicted, the positions of candidate stars are based on the obtained catalog, with typical errors of 20 mas. This precision is more than enough for a successful record of an occultation by Pluto, as its current apparent radius in the sky is about 50 mas. However, Nix and Hydra are more subject to missings, as their apparent radii are about 7 mas only.

3. Observations at ESO

Observations were made at the 2.2 m Max-Planck ESO (ESO2p2) telescope (IAU code 809) using the Wide Field Imager (WFI) CCD mosaic detector. Each mosaic is composed by eight 4k x 2k CCDs of $7.'5$ x $15'$ (RA, DEC) size, resulting on a total coverage of $30'$ x $30'$ per mosaic. Pixel scale is $0.''238$. A broad-band R filter (ESO#844) was used with $\lambda_c = 651.725$ nm and $\triangle\lambda = 162.184$ nm (full width at half maximum). Exposure time was 30^s. In very few cases, to compensate for non-ideal weather conditions, larger exposure times were used. In general, S/N ratios of about 200 were reached to objects with $R = 17$ without saturating bright ($R = 13$–15) stars. Limiting magnitude was about

Fig. 1. Sky path covered by the ESO2p2/WFI CCD mosaic observations. Years 2008–2015 follow from top to bottom. Each dashed form represents the 30′ x 30′ area covered by one single WFI mosaic. Note the gaps when, as seen from Earth, the Sun is too close to Pluto′s direction at date (no occultation could then be seen).

R = 21, with completeness about R = 18.0–19.0. Seeing varied between 0.″6 and 1.″5, being typically 1″.

Observations spanned Pluto′s sky path from 2008 to 2015. Runs were carried out in September and October 2007, covering respectively 2008–2010 and 2011–2015 paths. Mosaic overlapping was optimized for astrometric precision and telescope time consuming, including small shifts so that each star was exposed at least twice in different CCDs. Table 1 lists the WFI mosaic centers for each covered year. A total of 150 WFI mosaics or 1200 individual CCD frames were acquired for science. This resulted in about 40GB of photometrically calibrated processed images.

Fig. 1 illustrates the sky path covered. Years 2008–2015 follow from top to bottom. Dashed forms represent the 30′ x 30′ area covered by each single WFI mosaic in the sky plane. Note the gaps, when as seen from Earth, the Sun is too close to Pluto′s direction at date (no occultation could then be seen).

In all - including the 150 science mosaics for Pluto - 398 observed WFI mosaics (170 in September, 228 in October 2007) or 3184 individual CCD frames were used for determining astrometric field distortions (see Sect. 4.1), resulting in about 108GB of photometrically calibrated processed images. The mosaic centers were distributed along the projected Galactic plane, next to Pluto′s sky paths, where the star-crowded fields particularly favour resolution of distortion maps. The 248 extra mosaics served for another similar astrometric program carried out at the same instrument, covering the 2008–2015 sky path of transneptunian Quaoar, close to Pluto′s own sky path.

4. Astrometry

All CCD images underwent overscan, zeromean, flatfield and bad pixel corrections with IRAF (Tody 1993) via esowfi (Jones and Valdes 2000) and mscred (Valdes 1998) packages. Using the PRAIA package, the astrometric treatment consisted of three steps. First, a Field Distortion Pattern

was determined for each CCD in the WFI mosaics for each run. Then, astrometry was performed over the individual CCDs, with the (x, y) measurements corrected by the pre-determined field distortions. Next, all positions of common objects observed over the different CCDs and mosaics are combined in a global solution for each year, when final (RA, DEC) star positions are obtained. Besides positions, proper motions are also computed for each object using the 2MASS and USNO B1.0 catalogs as first epoch. These procedures are described in detail in the following subsections.

4.1. Field Distortion Pattern

Field Distortion Pattern (FDP) is characterized by existence of at least two different regions on the CCD field where fixed distances on the sky present different angular distance measurements, even after modeling known astronomical effects (differential refraction, etc). The ESO2p2/WFI mosaic is affected by FDP due to optical distortions of third order, which may reach more than twice the size of a pixel (0.″238).

The procedure for mapping the distortions for each CCD of the WFI mosaic started by superposing the observed minus catalog (O−C) position differences of UCAC2 stars computed from the respective individual CCD astrometric solutions of the 398 WFI mosaics observed nearby the projected Galactic plane and along Pluto′s sky path (see Sect. 3). For each CCD, these (O−C) position residuals were averaged over bins of 1.″5 x 1.″5 in (x, y). About 1035 position residuals were available per bin. Afterwards, in an iterative process, part of the averages were successively applied as a correction to the distortion. The procedure continued until no significant change occurred in the (O−C) residuals. Independent FDPs were computed for each observation run in September and October 2007. Note that only polynomials of first order are used to relate the (x, y) measurements with the UCAC2 star coordinates projected in the sky plane. In this way, the third order distortions are consistently mapped onto the FDP. This allows for the use of first degree polynomials in the individual CCD frame reductions, instead of third order ones, after first applying FDP corrections. The use of simpler polynomials improves position accuracy, as it increases the ratio between the number of reference stars over the number of coefficients used in the model.

The (Δx, Δy) FDP offsets for each (x, y) bin and CCD from the WFI mosaics of the September and October 2007 runs were computed and stored. The FDP offsets are available under request to the author. Figure 2 illustrates the FDP derived from the September 2007 run for each CCD in the WFI mosaic. North is up, East is left. CCDs are numbered from 1 to 8. By convention, from East to West are North CCDs 1 to 4. From West to East are South CCDs 5 to 8. The largest offset (upper-right corner of plot) is 528 mas. Similar plot is obtained for the October 2007 run. The astrometric procedures used to derive the (RA, DEC)s that feed the FDP computation were the same as those described next in Sect. 4.2.

4.2. Astrometry of individual CCD frames

After obtaining the FDPs, we have computed (RA, DEC)s for all stars measured in the CCDs of all the observed mo-

Table 1. The (α,δ) ESO2p2/WFI mosaic centers for Pluto sky path from 2008 to 2015.

Year	2008			2009			2010			2011			2012			2013			2014			2015		
	h	m	° ′	h	m	° ′	h	m	° ′	h	m	° ′	h	m	° ′	h	m	° ′	h	m	° ′	h	m	° ′
	18	02	-17 10	18	09	-17 46	18	18	-18 19	18	27	-18 50	18	35	-19 20	18	43	-19 48	18	51	-20 14	18	59	-20 38
	18	03	-17 09	18	10	-17 46	18	19	-18 19	18	28	-18 49	18	36	-19 19	18	44	-19 47	18	52	-20 13	19	00	-20 37
	18	04	-17 07	18	11	-17 45	18	20	-18 18	18	29	-18 49	18	37	-19 18	18	45	-19 46	18	53	-20 12	19	01	-20 36
	18	01	-17 03	18	12	-17 44	18	21	-18 17	18	30	-18 47	18	38	-19 17	18	46	-19 45	18	54	-20 11	19	02	-20 35
	18	00	-17 03	18	13	-17 42	18	22	-18 15	18	31	-18 45	18	39	-19 16	18	47	-19 44	18	55	-20 10	19	03	-20 34
	17	59	-17 04	18	08	-17 41	18	17	-18 17	18	30	-18 45	18	39	-19 15	18	48	-19 43	18	56	-20 09	19	04	-20 33
	17	58	-17 05	18	07	-17 42	18	16	-18 18	18	29	-18 46	18	38	-19 16	18	47	-19 44	18	57	-20 08	19	05	-20 32
	17	57	-17 06	18	06	-17 44	18	15	-18 20	18	28	-18 47	18	37	-19 18	18	46	-19 46	18	56	-20 10	19	04	-20 36
	17	56	-17 08	18	05	-17 46	18	14	-18 21	18	27	-18 48	18	36	-19 19	18	45	-19 48	18	55	-20 12	19	03	-20 38
	17	55	-17 10	18	04	-17 48	18	13	-18 24	18	26	-18 50	18	35	-19 21	18	44	-19 50	18	54	-20 14	19	02	-20 41
	17	54	-17 14	18	03	-17 52	18	12	-18 27	18	25	-18 51	18	34	-19 23	18	43	-19 51	18	53	-20 16	19	01	-20 43
	17	54	-17 29	18	02	-17 59	18	11	-18 37	18	24	-18 53	18	33	-19 24	18	42	-19 54	18	52	-20 18	19	00	-20 45
	17	55	-17 33	18	04	-18 10	18	12	-18 42	18	23	-18 55	18	32	-19 27	18	41	-19 56	18	51	-20 21	18	59	-20 48
	17	56	-17 36	18	05	-18 12	18	13	-18 45	18	22	-18 58	18	31	-19 29	18	40	-19 58	18	50	-20 23	18	58	-20 50
							18	14	-18 47	18	21	-19 01	18	30	-19 32	18	39	-20 01	18	49	-20 25	18	57	-20 53
							18	15	-18 48	18	20	-19 07	18	29	-19 37	18	38	-20 05	18	48	-20 28	18	56	-20 56
										18	21	-19 15	18	29	-19 44	18	38	-20 14	18	47	-20 32	18	55	-21 00
										18	22	-19 18	18	30	-19 47	18	39	-20 16	18	46	-20 38	18	55	-21 06
										18	23	-19 19	18	31	-19 48	18	40	-20 17	18	47	-20 42	18	56	-21 07
										18	24	-19 20	18	32	-19 49	18	41	-20 17	18	48	-20 43	18	57	-21 07
													18	33	-19 50	18	42	-20 17	18	49	-20 43	18	58	-21 07
																			18	50	-20 43			
																			18	51	-20 43			

Each overlapping WFI mosaic encompass a 30′ x 30′ area in the sky. Sky paths 2008–2010 and 2011–2015 were observed in September and October 2007 runs, respectively.

saics covering the sky paths from 2008 to 2015. The (x, y) measurements were pre-corrected with the FDP of the respective run, according to the respective bin and CCD in the WFI mosaic. Correction values were extrapolated by the inverse square distance to neighbour bin centers.

Positions were obtained using PRAIA (Assafin 2006). This fast astrometric/photometric package automatically identifies objects on the fields. The (x, y) measurements are performed with 2–dimensional circular symmetric Gaussian fits within 1 Full Width Half Maximum (FWHM = seeing). Within 1 FWHM, the image profile is well described by a Gaussian profile, free from wing distortions which jeopardize center determination. Theoretical and empirical results support this procedure (Moffat et al. 1969; Stone, R. 1989). PRAIA automatically recognizes catalog stars and determines (RA,DEC) with a number of models relating the (x, y) measured and (X, Y) standard coordinates projected in the sky tangent plane. Positions, (x, y) centers, magnitudes, seeing - among other quantities and respective estimated errors - are computed and archived for all objects.

Magnitudes were obtained from PSF photometry and were calibrated with respect to the UCAC2. Note that the UCAC2 star magnitudes are based on a 579-642 nm filter (between Johnson V and R), thus distinct from the filter used in the WFI observations. Thus, the image-to-image magnitude zero point will depend on the mean color of the field stars. However, since the photometric errors of the UCAC2 are somewhat large (about 0.3), we will consider here, for all purposes, that the derived WFI magnitudes are formally in the UCAC2 system. This issue will be further addressed after future releases of the UCAC catalog, when more refined photometric magnitudes are expected to be available. Furthermore, for simplicity, herein we will simply refer to WFI magnitudes as R magnitudes.

A complete and detailed description of the PRAIA package will be published in the future. See further details about performance in Assafin et al. (2007).
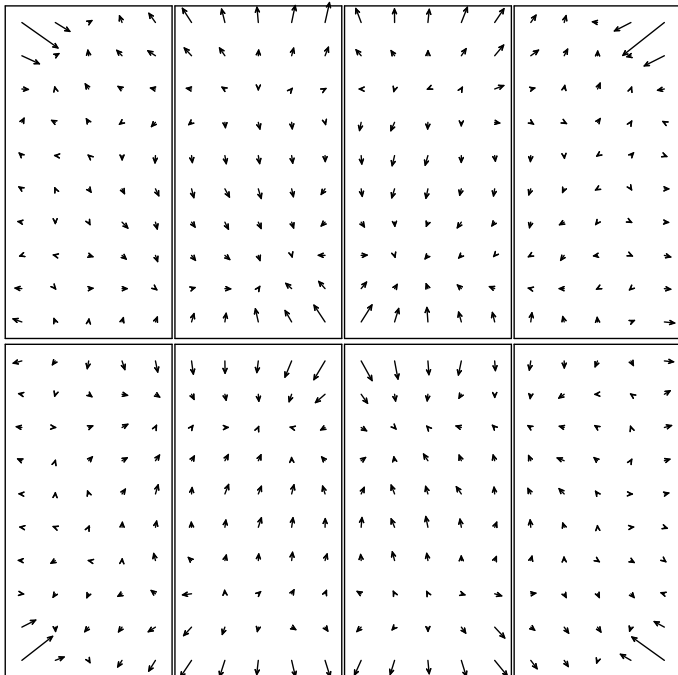
We used the UCAC2 as reference frame and the 6 constants polynomial to model (x, y) measurements to (X, Y) plane coordinates. About 120 UCAC2 stars per frame were used in these Galactic plane star-crowded fields. Reference stars were eliminated in a one-by-one basis until none displayed (O−C) position residuals greater than 120 mas (2–3σ the typical catalog error). The position mean errors from (RA, DEC) solutions were about 60mas for both coordinates. Estimated (x, y) measurement errors from Gaussian fits were about 20 – 30 mas between $12 < R < 17$, rising as expected at magnitudes brighter and fainter than this range. Fig. 3 shows the distribution of (x, y) errors as a function of R magnitude. Values were averaged over 0.5 magnitude bins from all measured CCDs.

A summary of the results from the individual CCD astrometric treatment is given in Table 2. For each year, we list the number of CCD frames, mean error of positions from (RA, DEC) solutions and average number of UCAC2 reference stars per frame.

The same procedures here described were applied to individual CCD fields for obtaining the FDPs (Sect. 4.1).

4.3. Mosaic global astrometric solution

For each year, global astrometric solution for overlapping mosaics of CCDs was accomplished by an iterative procedure available by PRAIA. Starting from the individual CCD measurements (see Sect. 4.2), all common star positions, magnitudes and other values and errors were averaged. Common stars were recognized among CCD frames by individual CCD positions laying within 200 mas from each other. Then, a method which we call Tangent Plane
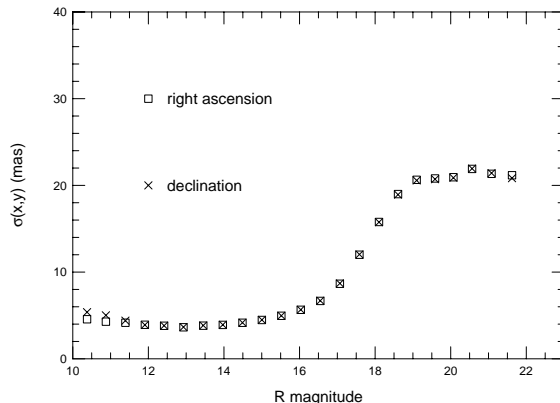
Fig. 2. Field Distortion Pattern (FDP) for the 8 CCDs of the WFI mosaic for the September 2007 run. North is up, East is left. From East to West are North CCDs 1 to 4. From West to East are South CCDs 5 to 8. Arrows point to the FDP-corrected position. The largest one (upper-right corner of plot) is 528 mas. Bins have 1′.5 x 1′.5 sizes. Averaged values come from the contribution of individual (O−C) position differences of UCAC2 stars obtained from astrometry of 398 WFI mosaics observed nearby the projected Galactic plane and along Pluto′s sky path (see Sect. 3). On average, there were 1035 (O−C) position residuals available per bin. A similar FDP is found for the October 2007 run. See details of FDP computation in Sect. 4.1.

Table 2. Astrometry of individual CCD frames of WFI mosaics.

Sky path Year	Mean errors		Frames per year	No. UCAC2 stars/frame
	$\sigma(\Delta\alpha\cos\delta)$ mas	$\sigma(\Delta\delta)$ mas		
2008	59	59	112	105
2009	58	56	112	79
2010	58	56	128	164
2011	61	59	160	153
2012	63	62	168	125
2013	63	62	168	107
2014	62	62	184	105
2015	58	57	168	132

Average mean errors come from standard deviations of (O−C) residuals from individual (RA, DEC) solutions with the UCAC2 catalog. The 6 constants polynomial model was used to relate (x, y) measurements with (X, Y) tangent plane coordinates. The (x, y) centers were pre-corrected by the FDPs. See details in Sect. 4.2.

Technique, adapted from Assafin et al. (1997), was applied. In this method, all the CCD frame (RA, DEC)s and catalog-extracted UCAC2 reference positions (corrected by proper motions to the mean epoch of observations) are projected in the tangent plane. A complete polynomial model of the third degree is then used to relate these projected coordinates in the same way as in classical photographic field astrometry. After the elimination of UCAC2 stars out-

Fig. 3. (x, y) measurement errors as a function of R magnitude from all treated CCDs. Values are averages over 0.5 magnitude bins.

liers with (O−C) residuals larger than 120 mas, the tangent plane solution was obtained. Inverse gnomonic projection furnished the (RA, DEC) of all objects in the mosaic. These positions formed an intermediary star catalog in the UCAC2 reference frame. Next, new individual CCD astrometric adjustments were performed, but now using this intermediary catalog as reference frame for all CCD fields. Now, every star in the individual CCD frames participates as reference star. Here, a complete third degree polynomial model was used (instead of the 6 constant model used in the first step in Sect. 4.2) and new individual CCD positions were obtained. The entire process was then repeated in an iterative fashion, with new averaging of common positions and new application of the Tangent Plane Technique. The procedure stopped after intermediary catalog star positions converged to within 1 mas, which always happened in less than 50 iterations.

Table 3 brings a summary of the results from the global solutions of WFI CCD mosaics for the sky path observed, focusing on the Tangent Plane Technique results. For each year, it gives the standard deviations (σ) of observed minus UCAC2 catalog positions, before and after the global solution. The listed zero-point position offsets were computed from averaged (RA, DEC) offsets over UCAC2 stars, before applying the global mosaic solution. By definition, due to the Tangent Plane Technique, after global solution they are zero. Table 3 also brings the number of UCAC2 reference stars used in the process.

4.4. Star multiplicity

About 8% of stars displayed multiple position entries within 1″.5 of each other after global mosaic solutions. This happened whenever individual CCD positions from the same object did not pass the 200 mas criterium for identification of common stars in the global solution procedure. As a result, multiple positions survived the proccess as if they belonged to distinct objects. In the vast majority of cases, these entries displayed magnitudes fainter than R = 19. The

Table 3. Global astrometric solution for WFI CCD mosaics. Tangent Plane Technique results.

Sky path	Zero-point offset before G.S.		(RA,DEC)–UCAC2				UCAC2 stars
	$\Delta\alpha\cos\delta$	$\Delta\delta$	before G.S.		after G.S.		
	mas	mas	σ_α	σ_δ	σ_α	σ_δ	
Year			mas	mas	mas	mas	
2008	-13	-04	112	107	59	58	6001
2009	-09	-01	112	103	58	55	4693
2010	-03	-03	133	126	59	57	11013
2011	-08	-03	134	129	61	59	8988
2012	-06	-05	139	131	62	61	7563
2013	-03	-04	145	141	63	62	6068
2014	-06	$+02$	135	138	60	60	6439
2015	-06	-03	100	098	57	57	7524

Zero point position offsets were computed from averaged observed minus UCAC2 star position differences, before applying the global mosaic solution procedure (G.S.). Due to the Tangent Plane Technique, by definition they are zero after G.S. process. The $(\sigma_\alpha, \sigma_\delta)$s of Tangent Plane Technique solutions refer to observed minus UCAC2 positions computed before and after G.S procedure. Last column is the number of used UCAC2 reference stars (see details in Sect. 4.3).

Table 4. Multiplicity flags for WFI global mosaic star positions.

	UCAC2		2MASS		Field		No	Input
	f1	f2	f1	f2	f3	f4	flag	entries
Year	%	%	%	%	%	%	%	
2008	0.0	0.0	1.4	0.7	1.0	2.6	94.3	296,823
2009	0.1	0.0	5.2	3.1	0.3	1.5	89.8	53,221
2010	0.0	0.0	0.4	0.6	1.3	1.6	96.1	378,236
2011	0.0	0.0	0.7	0.7	2.9	1.9	93.8	502,966
2012	0.0	0.0	0.3	0.8	3.1	2.1	93.7	672,564
2013	0.4	0.0	9.8	3.3	1.1	3.1	82.3	201,541
2014	1.8	0.1	13.0	4.7	2.1	3.5	74.8	159,725
2015	0.0	0.0	1.3	0.6	3.8	3.1	91.2	194,573

Input entries give the number of mosaic positions before checking for multiplicity. Multiplicity flag percentages refer to the final number of positions, one per object. No flag (good astrometry) means no multiple entries within $1''\!.5$ for the same object after mosaic solutions. Flag cases f1 and f2 apply only for UCAC2 and 2MASS stars, when only entries assigned to a catalog are used. Flag f1 means that more than one entry was used, flag f2 indicates that only one entry was used. Flags f3, f4 and f5 apply only to field stars and mean only one entry was selected according to one of three criteria, in order of priority: a) highest number of used common individual CCD positions (flag f3); b) least (x, y) measurement error (flag f4); c) brightest R magnitude (flag f5). Percentage of flag f5 entries is always less than 0.1% and thus is not displayed.

cause might be poor faint star deblending in the individual CCD frame (x,y) measurements, as heavily star-crowded sky fields were sampled. Stars with multiple entries were assigned one unique position and flagged. No flag means star with no multiple entries (good astrometry). Flag cases f1 and f2 apply only for UCAC2 or 2MASS stars. In these cases, multiple entries assigned to one of these catalogs were used, but others wrongly assigned as field stars were rejected. Flag f1 means that more than one entry was used, flag f2 indicates that only one entry was used. Flags f3, f4 and f5 apply only for field stars. Only a single entry was selected according to one of three criteria, in order of priority: a) highest number of used common individual CCD positions (flag f3); b) least (x, y) measurement error (flag f4); c) brightest R magnitude (flag f5).

Table 4 displays multiplicity flag statistics for the derived ESO2p2/WFI global mosaic star positions, according to catalog and year. The input number of unflagged entries is furnished, but percentages refer to the final number of WFI stars. Percentages for flag f5 entries were always less than 0.1% and thus are not displayed.

After checking for multiplicity and flagging, the final set of global mosaic star positions is obtained. For the flagged stars, magnitude, mean epoch and other parameters were assigned in the same way as for positions, but no position error could be estimated for them.

4.5. Computation of proper motions

One important step in our astrometric procedure was the derivation of proper motions for stars not belonging to the UCAC2, using the 2MASS and USNO B1.0 catalogs as first epoch. The mean epochs of the 2MASS and USNO B1.0 catalogs are respectively around 2000 and 1980. The 2MASS catalog is based on infrared bandpass observations with modern solid state detectors. USNO B1.0 was created from astrometric digitalization of photographic Schmidt plates. 2MASS position precision ranges between 100-200 mas, better than the 250-300 mas errors of USNO B1.0 positions. But, time span favours USNO B1.0, so that the overall at-

tained error budget of computed proper motions is similar, regardless of the first epoch used.

In the procedure, the first epoch position for brighter stars was chosen from the 2MASS. If the star was fainter - that is, did not belong to that catalog - then the USNO B1.0 position was used, instead. For both catalogs, only matches within $1''$ in position were considered. No brightness constrains were applied for matching the USNO B1.0. For the 2MASS case, stars with discrepancies higher than 1 magnitude were rejected in comparing measured R magnitudes with H band. For multiple matches, the closest magnitude was selected.

In Table 5, we give a summary of the proper motion computations using the WFI global mosaic star positions, 2MASS and USNO B1.0 catalogs. For each year, we list the total number of final global mosaic star positions, the number of UCAC2 stars with proper motions (directly extracted from UCAC2), number of stars with proper motions based on the 2MASS and USNO B1.0 and number of non-matched stars, for which no proper motion could be computed. Again, cases where no proper motion could be derived relate almost exclusively to stars fainter than R = 19.

5. The catalog of star positions along Pluto's 2008-2015 sky path

The star catalog for the 2008–2015 sky path of Pluto consists of mean (RA, DEC) positions in the ICRS (J2000), proper motions, R magnitudes (also J, H and K in the case of 2MASS stars), mean epoch of observations, position error at mean epoch of observation and magnitude error estimates. It has 2,242,286 stars in the UCAC2 frame. Its mean epoch is approx. 2007.75. Magnitude completeness is about R = 18–19. Magnitude limit is about R = 21. Position error is about 50 mas for stars up to magnitude R = 19, and

Table 5. Proper motion computations from 2MASS, USNO B1.0 and ESO2p2/WFI global mosaic star positions.

Year	final mosaic positions	UCAC2 p.m.	2MASS p.m.	USNO B1.0 p.m.	No p.m.
2008	279,127	9,826	155,807	47,774	65,72
2009	47,576	7,343	32,213	5,472	2,548
2010	361,830	20,704	121,440	69,433	150,2!
2011	466,433	17,740	167,283	83,910	197,50
2012	622,343	15,689	155,970	128,038	322,64
2013	166,283	14,180	109,182	20,722	22,19
2014	122,199	13,634	78,610	14,985	14,97
2015	176,495	11,067	72,908	37,607	54,91
total	2,242,286	110,183	893,413	407,941	830,74

Number of final global mosaic star positions, number of UCAC2 stars with proper motions (directly extracted from UCAC2), number of stars with proper motions based on the 2MASS and USNO B1.0 and number of stars for which no proper motion could be computed.
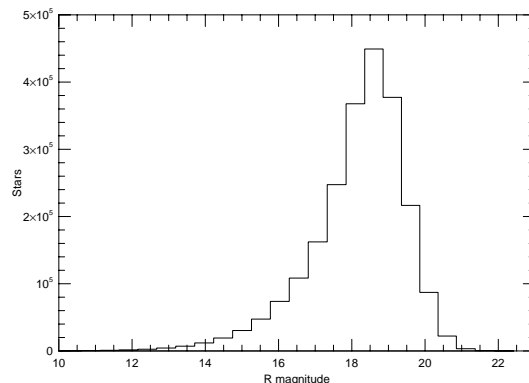

Fig. 4. Star distribution per R magnitude. It illustrates the R magnitude limit and completeness of catalog. Counts were computed over 0.5 magnitude bins.

25 mas up to R = 17. The catalog is freely available in electronic form via anonymous ftp to cdsarc.u-strasbg.fr.

The catalog is divided by year. There are small gaps between the years (see Fig. 1). Stars which had multiple entries within $1''5$ in the global mosaic solutions (about 8% of total) are flagged (see Sect. 4.4). R magnitudes from PSF photometry were calibrated in the UCAC2 system, so magnitude zero-point errors up to 0.3 might be expected for R > 17. Position error is estimated from repeatability, by the standard deviation (mean error) of contributing individual CCD positions about the final catalog star positions (last iteration in global mosaic solution - see Sect. 4.3). By default, multiple entry flagged stars have no position error estimates. Infrared magnitudes (and errors) were extracted from the 2MASS catalog. Error estimates for R magnitudes come from the standard deviation about the mean from individual CCD frames. Sky coverage of the catalog is detailed in Sect. 3.

Table 6 lists the total number of catalog stars per year, average position errors, R bandpass magnitude limit (including highest values) and completeness. Fig. 4 shows the star distribution per R magnitude. Fig. 5 plots the position error as a function of R magnitude. Values were averaged over 0.5 magnitude bins.

6. Pluto's ephemeris offsets

In the recent past, a number of stellar occultations by Pluto and Charon have then been foreseen for 2005–2008. The successful outcome of such complex international observational campaigns were only actually achieved thanks to precise position updates for the candidate stars, starting long enough in advance and continued until the epoch of those events. Most of those prediction updates have come from the astrometric observational program of Pluto carried out at the 0.6m B&C telescope at the Laboratório Nacional de Astrofísica (LNA), Brazil (IAU code 874). Those observations were made with $1k^2$ and $2k^2$ CCD detectors of $10'$ sizes and pixel scales of $0''3$ to $0''6$ (for a detailed description of telescope/instruments, see Assafin et al. 2005). The PRAIA package was employed in the astrometry of these CCD observations. Frames were free from high order optical distortions and were modeled with 6 constant polynomials. Typical (x,y) measurement errors were about

15 mas for R < 15. Position mean errors from astrometric (RA, DEC) solutions ranged between 50–60 mas. Position precision inferred from the repeatability of solutions was about 20 mas. Positions were referred to the UCAC2 catalog. The UCAC2-based candidate star positions were zero-point-corrected toward ICRS, using averaged UCAC2 minus ICRF position offsets of $\Delta\alpha\cos\delta$ = -12 ±8 mas and $\Delta\delta$=−5 ±7 mas. These local offsets were computed from the comparison between optical and VLBI positions for the 5 nearest ICRF quasars to Pluto's 2006.5 coordinates, distributed within 10 degrees radius (see Assafin et al. 2005). Table 7 summarizes the astrometry of candidate stars with the 0.6m LNA telescope for 2005–2008 Pluto stellar occultations. Only results regarding final positions used for deriving ephemeris offsets are displayed. They refer to observations made at least within a month of event epoch. One exception was the 12 June 2006 event, for which good CCD observations were only available from an April 2007 run. As it was a UCAC2 star, the derived CCD position could be referred to the epoch of event by applying UCAC2 proper motions. The 25 August 2008 event star was observed with the 1.6m P&E LNA telescope (FOV of $5' \times 5'$ and pixel scale of $0''17$).

Observations of Pluto itself were made in a regular basis and also prior to the events with the 0.6m B&C LNA telescope, for estimating possible ephemeris offsets. More than 1,500 Pluto positions where obtained in the time span between 2005–2008, following the same observational and astrometric procedures. These Pluto positions were accurate enough to display the perturbation by Charon, although it was unresolved in the CCD images. We usually solved this problem by looking at the (O−C) ephemeris residuals from observations symmetrically distributed along the 6.4-day orbital period of Charon. Later on, a new procedure for determining position offsets was implemented, which allowed the use of all observations. This new method is based on the modeling of the resulting PSF of unresolved images, in terms of relative apparent distance between components, relative brightness and seeing conditions.

Table 6. Star catalog for the 2008–2015 Pluto sky path.

Year	2008	2009	2010	2011	2012	2013	2014	2015
catalog stars	279,127	47,576	361,830	466,433	622,436	166,283	122,199	176,495
UCAC2 stars	9,826	7,343	20,704	17,740	15,689	14,180	13,634	11,067
2MASS stars	155,834	32,217	121,489	167,309	155,998	109,201	78,623	72,926
Field stars	113,467	8,016	219,637	281,384	450,656	42,902	29,942	92,502
σ_α (mas)	25	27	24	27	25	31	33	30
σ_δ (mas)	24	23	22	24	24	36	39	29
highest R magnitude	22.7	22.3	23.4	22.5	23.7	22.3	21.8	24.0
R magnitude limit	21.0	21.0	21.5	21.0	21.5	21.0	21.0	21.5
R magnitude completeness	9.5-18.5	8.5-18.0	9.5-18.5	10.0-19.0	10.4-19.0	9.1-18.0	8.5-18.0	9.4-18.5

Number of catalog stars per year, position error (estimated from the standard deviation of contributing individual CCD positions about the final catalog star positions), R bandpass magnitude completeness, magnitude limit and highest value.

Table 7. Astrometry of candidate stars observed at the 0.6m B&C LNA telescope for 2005–2008 Pluto stellar occultations.

Event	(RA, DEC) Epoch years	ICRS (J2000) (RA, DEC) h m s ° ′ ″	Magnitude (R)	Error E_α mas	Error E_δ mas	No. Obs.	Mean Error σ_α mas	Mean Error σ_δ mas	UCAC2 stars No.
11 July 2005	2005.2560	17 28 55.0167 -15 00 54.726	14.9	11	15	25	50	52	66
10 April 2006	2006.1620	17 46 06.8788 -15 46 10.113	16.0	33	32	255	56	55	107
12 June 2006	2006.4449	17 41 12.0769 -15 41 34.488	15.0	11	15	13	61	59	186
18 March 2007	2007.2165	17 55 05.6948 -16 28 34.369	15.1	08	11	12	59	62	162
12 May 2007	2007.3641	17 53 32.1024 -16 22 47.359	16.5	56	30	8	57	58	176
09 June 2007	2007.4598	17 50 50.6520 -16 22 29.309	17.0	16	03	4	56	60	94
14 June 2007	2007.4588	17 50 20.7402 -16 22 42.207	15.6	48	54	190	58	55	108
31 July 2007	2007.4634	17 45 41.9894 -16 29 31.639	14.0	15	24	68	60	56	72
22 June 2008	2008.4044	17 58 33.0147 -17 02 38.340	13.5	11	09	50	50	48	76
24 June 2008	2008.4044	17 58 22.3941 -17 02 49.346	15.9	13	17	50	50	48	76
25 August 2008	2008.6494	17 53 27.1040 -17 15 27.541	15.6	06	04	30	56	56	26

Used positions are always within a month of event epoch. Error estimates come from the dispersion (standard deviation) of values from the observations. Mean error of (RA, DEC) solutions and average number of UCAC2 reference stars are given. The UCAC2-based candidate star positions were zero-point-corrected toward ICRS using averaged UCAC2 minus ICRF position offsets ($\Delta\alpha\cos\delta = -12 \pm 8$ mas; $\Delta\delta = -5 \pm 7$ mas) of 5 ICRF quasars nearby Pluto present coordinates (see Assafin et al. 2005). For the 12 June 2006 event, useful CCD observations were only acquired in April 2007, but the final position is at event epoch, as proper motions ($\mu_\alpha = -10.6$ mas yr^{-1}, $\mu_\delta = -12.9$ mas yr^{-1}) were applied for this UCAC2 star. The 25 August 2008 event star was observed with the 1.6m P&E LNA telescope (FOV of 5′ sizes and pixel scale of 0″17).
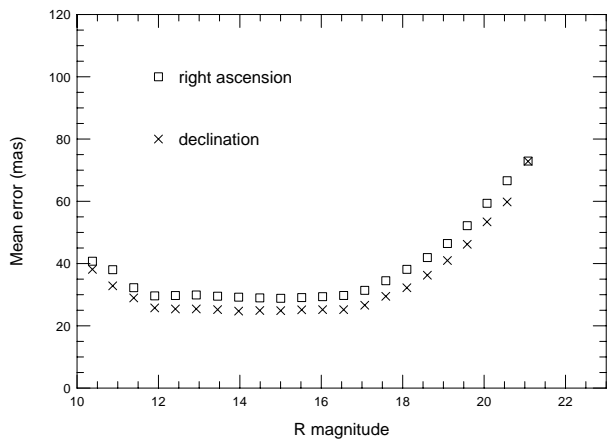
This ephemeris checking procedure proved to be very important for the successful recording of these past occultations. The predicted Earth locations would be severely misplaced if ephemeris offsets mostly in declination were not properly taken into account in advance, during the campaign planing phase. Indeed, based on these LNA observations, we have not only started to find large offsets of some tens of mas but, as time went by, we have also detected evidence of a linear ephemeris drift in declination for Pluto. Details of these results will be published elsewhere (Vieira Martins et al. 2009).

In a stellar occultation with two or more observed cords, Pluto′s position relative to the occulted star can be derived with mas-level accuracy. If the star position is known, Pluto′s right ascension and declination ephemeris offsets can be determined for that instant. A collection of ephemeris offsets obtained over time helps determining systematic trends, if present.

After fitting synthetic light curves to observations of the events listed in Table 7 (Sicardy et al. 2009) and taking into account the respective star positions, Pluto′s offsets relative to its ephemeris were computed. Here, the DE418 and plu017 ephemerides were used, as they were specially devised for the New Horizons mission to Pluto (Folkner et al. 2007). They are available through NASAs Navigation and Ancillary Information Facility (NAIF) ftp

site (ftp://naif.jpl.nasa.gov/pub/naif/) as SPICE kernels DE418 and plu017 (see details about NAIF in Acton 1996). The ephemeris offsets obtained for each event are listed in Table 8. For the 10 April 2006 event, no occultation occurred (this was actually predicted), but the offset could be derived (at 20 mas level) due to high resolution adaptive optics observations of Pluto and star made at the ESO-VLT 8m Telescope UT4 (Yepun) at Paranal Observatory, Chile, with the NACO instrument. The event of 11 July 2005 involved Charon, while the event of 22 June 2008 involved both Pluto and Charon occulting the same star. In all other cases, the events concern stellar occultations by Pluto alone. Table 8 also lists 4 extra offsets measured for 4 common events, based on an independent set of star positions and occultation observations (Young et al. 2008; Young et al. 2007; Olkin et al. 2009; Buie et al. 2009). Averaged offsets from this independent set with our derived values are also furnished for these 4 common events.

From Table 8, a clear linear drift with time is seen for the declination offsets. This drift must be taken into account in the predictions, as the occultation shadow path over the Earth is most sensitive to an ephemeris offset in declination. Thus, adopting the empirical relation *off-set* $= A * (t - 2005.0) + B$ with offsets in mas and time in years, and fitting the 12 declination offsets listed in Table 8

Fig. 5. Catalog position mean errors as a function of R magnitude. Position errors are estimated from the standard deviation of contributing individual CCD positions about the final catalog star positions (last iteration in global mosaic solution - see Sect. 4.3). Values were computed over 0.5 magnitude bins.

(only averaged values were used in the case of the four common events), we find $(A, B) = (+30.5 \pm 4.3 \text{ mas yr}^{-1}, -31.5 \pm 11.3 \text{ mas})$, with an (O−C) standard deviation of 14.4 mas for the offsets. Figure 6 plots the $(\Delta\alpha\cos\delta, \Delta\delta)$ ephemerides offsets (DE418 and plu017) of Pluto against time for the 12 studied occultations. The fitted linear drift with time in declination is illustrated.

From Fig. 6 it can be seen that the ephemeris offsets in right ascension are more dispersed than in declination. One might try to explain it by the appealing scenario of an oscillation pattern related to an error in Pluto's heliocentric distance (geocentric parallax error). However, contrary to declination, none of the attempted models for this scenario could fit the offsets well below 50 mas standard deviation, particularly for the events in opposition - even after introducing an empirical linear drift with time in right ascension. This issue will be further addressed in detail in a forthcoming paper (Vieira Martins et al. 2009). In the present work, we have not applied offset corrections of any kind to right ascension. This is here justified by the pragmatic fact that the eventual presence of right ascension ephemeris offsets do not affect the geographic latitude of Pluto's shadow path over the Earth, except - and only marginally so - far from opposition. Usually, it will only cause a slight error in the predicted central instant of the occultation by a few minutes at most, which from the observational point of view is usually easily accommodated by extending the duration of the occultation run.

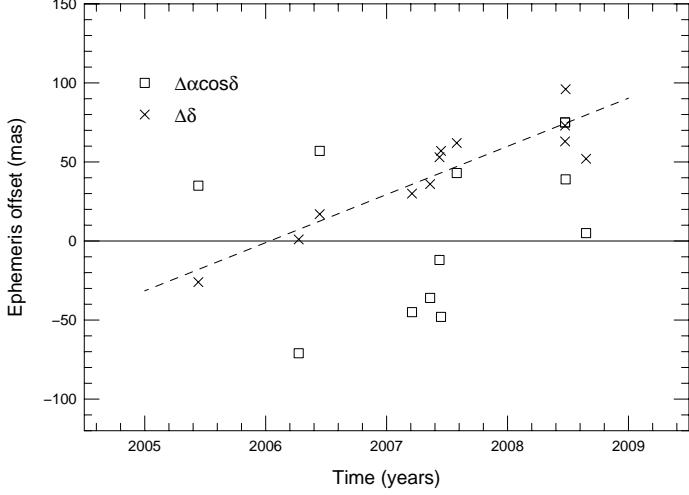**Table 8.** Pluto DE418 and plu017 ephemerides offsets with time.

Event	Central Instant years	Observed - Ephem. $\Delta\alpha\cos\delta$ mas	$\Delta\delta$ mas	Note
11 July 2005	2005.4433	+35	−26	p
10 April 2006	2006.2731	−73	+00	p
12 June 2006	2006.4468	+63	+19	p
12 June 2006	2006.4468	+49	+15	1
12 June 2006	2006.4468	+56	+17	a
18 March 2007	2007.2100	−48	+30	p
18 March 2007	2007.2100	−46	+30	2
18 March 2007	2007.2100	−47	+30	a
12 May 2007	2007.3597	−38	+36	p
09 June 2007	2007.4371	−14	+53	p
14 June 2007	2007.4499	−49	+57	p
31 July 2007	2007.5799	+42	+64	p
31 July 2007	2007.5799	+42	+61	3
31 July 2007	2007.5799	+42	+62	a
22 June 2008	2008.4758	+73	+63	p
22 June 2008	2008.4758	+73	+73	p
24 June 2008	2008.4803	+37	+96	p
25 August 2008	2008.6494	+02	+53	p
25 August 2008	2008.6494	+04	+52	4
25 August 2008	2008.6494	+03	+52	a

DE418 and plu017 ephemerides offsets of Pluto with time. Offsets marked "p" were determined from fittings of past occultations in 2005–2008, taking as reference LNA-based star positions (Table 7) derived for these events. Four extra offsets from four common events were also independently measured ("1" = Young et al. 2008; "2" = Young et al. 2007; "3" = Olkin et al. 2009; "4" = Buie et al. 2009); for these common occultations, averaged offsets with the corresponding "p" values are marked "a". The offsets are in the sense observed minus ephemeris. For the 10 April 2006 event, no occultation occurred (this was actually predicted), but the offset could be derived (at 20 mas level) due to high resolution adaptative optics observations of Pluto and star made at the ESO-VLT 8m Telescope UT4 (Yepun) at Paranal Observatory, Chile, with the NACO instrument. The event of 11 July 2005 involved Charon, while the event of 22 June 2008 involved both Pluto and Charon occulting the same star. In all other cases, the events concern stellar occultations by Pluto alone.
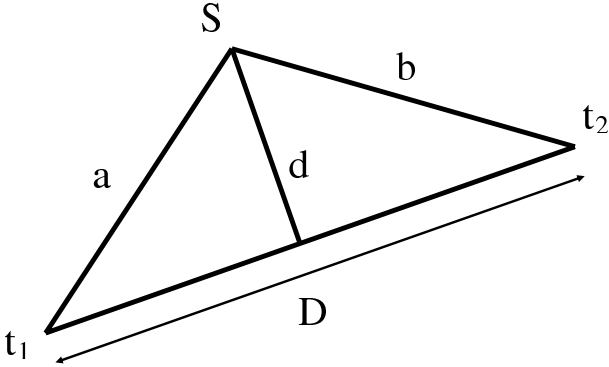
7. Search procedure for candidate stars

The search procedure for candidate stars to be occulted by Pluto and its satellites was based in the obtained star catalog described in Sect. 5, and by using the ephemeris drift derived for declination in Sect. 6. All catalog star positions, corrected by proper motions, were crossed against the DE418 and plu017 ephemerides of Pluto, Charon, Nix and Hydra, extracted in a per-minute basis for the whole period between 2008 to 2015. The body's declination ephemeris was offset according to the computed linear drifts for each instant. If the distance between the star position and the (offset-corrected) body ephemeris was less than a given value, then a potential occultation was found and all astrometric and geometric data relevant to the possible event was computed and stored.

For each candidate star, besides astrometric and photometric data, minimum apparent geocentric distance d, the central instant of closest approach t_0, shadow velocity v across the Earth, position angle PA of the shadow path and local solar time LST at sub-planet point were

Fig. 6. DE418 and plu017 ephemerides offsets of Pluto in right ascension and in declination against time in the sense observed minus ephemeris. Offsets were determined from fittings of past occultations in 2005–2008, taking as reference LNA-based positions derived for these stars (only averaged values were used in the case of the four common events listed in Table 8). The dotted line is the fitted linear drift in declination. No ephemeris offset correction was attempted for right ascension. (See discussion in the text of Sect. 6)

Fig. 7. Geometric configuration of potential close approach. a and b are the apparent geocentric distances in the plane of the sky between the body and the star at arbitrary instants t_1 and t_2 before and after the closest approach. D is the apparent geocentric distance between the body geocentric ephemeris positions at t_1 and t_2 and d is the minimum apparent geocentric distance at closest approach between the body and the star.

computed and stored. These geometric quantities were calculated as follows. Consider the close approach scheme displayed in Fig. 7, where a and b are the apparent geocentric distances in the plane of the sky between the star S and the body at arbitrary instants t_1 and t_2 before and after the

closest approach. D is the apparent geocentric distance between the body ephemeris positions at t_1 and t_2 and d is the minimum apparent geocentric distance at closest approach between the body and the star. The minimum apparent geocentric distance d is thus given by

$$d = \sqrt{a^2 - \left(\frac{a^2 - b^2 + D^2}{2D}\right)^2}$$

If $t_2 > t_1$, the central instant t_0 (UTC) of the occultations is

$$t_0 = t_1 + (t_2 - t_1)\sqrt{\frac{a^2 - d^2}{D^2}}$$

The velocity v in km s^{-1} of the shadow across the Earth at a distance A(km) from the body is given by

$$v = \frac{A\sin(D)}{(t_2 - t_1)}$$

with t_2 and t_1 expressed in seconds.

From the (offset-corrected) body's (RA, DEC) ephemeris and from the star position at t_0, one can easily calculate the position angle PA of the shadow path across the Earth surface at central instant t_0. It is defined as the position angle of the body with respect to the star at closest approach. PA is zero when the body is North of the star and is counted clockwise.

The rough local solar time LST at sub-planet point was computed by

$$LST = t_0 + long = t_0 + RA - MSTG$$

were $long$ is the east longitude of the sub-planet point, $MSTG$ is the Mean Sideral Time in Greenwich at t_0 and RA is the right ascension of the body at closest approach. Note that LST provides a rough indication as to whether the event is mostly observable during night time versus day time at the sub-planet point.

For the search, we have extracted ephemeris positions using 1 minute time intervals. After finding a potential occultation, however, we took ephemeris positions at t_1 and t_2 about 1h apart from each other, around t_0. This precaution allows for a significant change in the coordinates, thus improving computation precision, particularly far from opposition and close to stationary configurations, when shadow velocity v is small.

8. Predictions of stellar occultations by Pluto and its satellites

Following the procedure described in Sect. 7, candidate stars for occultations by Pluto, Charon, Nix and Hydra were found. The adopted search radius was 0″335 - about the apparent radius of Pluto (50 mas) plus the apparent Earth radius (285 mas) as projected in the sky plane at 31 AU (Pluto-Earth distance for 2008–2015). No predictions were discarded due to day light at sub-planet point, as occultations could, even so, be visible right above the horizon from places still in the dark near Earth terminator. For each body, all relevant astrometric, photometric and geometric information for each potential event found is

Table 10. Predictions for Pluto and its satellites for 2008–2015.

	2008	2009	2010	2011	2012	2013	2014	20
Pluto	148	26	184	239	333	90	71	1
Charon	147	27	195	238	325	88	77	1
Hydra	146	24	185	257	335	88	59	1
Nix	156	22	202	276	345	101	78	1

Number of predicted events per year for each body.

available in electronic form via anonymous ftp to cdsarc.u-strasbg.fr. Table 9 lists a sample of predictions for Pluto. It contains the date and instant of stellar occultation (UTC), the ICRS (J2000) star coordinates at the event date, the closest apparent geocentric distance between star and body, the position angle of the shadow across the Earth (clockwise, zero at North), the velocity in km s^{-1}, the distance to the Earth (AU), longitude of the sub-solar point, local solar time, DE418 and plu017 ephemerides offsets in (RA, DEC) for the central instant, catalog proper motion and multiplicity flags, estimated star catalog position errors, proper motions and magnitudes R*, J*, H* and K*. Magnitudes are normalized to a reference shadow velocity of 20 km s^{-1} by

$$M^* = M + 2.5 \, log_{10} \left(\frac{v}{20 \ km \ s^{-1}} \right)$$
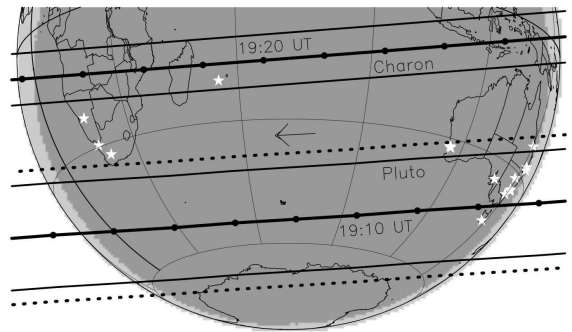
The value 20 km s^{-1} is typical of events around Pluto opposition. Therefore, M* may bring forward faint stars involved in slow events, thus allowing for longer integration time, and consequently reasonably good signal to noise ratios (SNRs) without loss of spatial resolution in diameter measurements and in probing atmosphere altitudes in the light curves, in spite of the faintness of the targets. Note, however, that Pluto's important contribution to the total recorded flux will the be an issue in those situations, so that a case by case estimation of SNR must be conducted for those candidates.

Figure. 8 illustrates the geometry of the 22 June 2008 event on Earth (see details in Table 9). As predicted, it was actually a double occultation of the same star by Pluto and Charon. The occultations were visible in South Australia, Namibia and La Reunion Island and were eventually recorded from five sites in Australia and one site in La Reunion Island in the Indian Ocean.

Table 10 displays the total number of predicted events for each body for the period 2008–2015.

9. Discussion

We presented predictions for stellar occultations by Pluto, Charon, Nix and Hydra for 2008–2015 based on observations made with the ESO2p2/WFI CCD mosaic. For that, an astrometric catalog of 2.24M stars with proper motions was derived encompassing the 2008–2015 sky path of Pluto within 30′ width. It is in the UCAC2 reference frame and has magnitude completeness about R = 18–19 with limit around R = 21. Its mean epoch is around 2007.75. Position error is about 25 mas for R = 12–17, ranging from 25 mas to 50 mas for R = 17–19 (Fig. 5). The entire astrometric catalog and the complete set of tables with stellar occultation predictions are available in electronic form via anonymous ftp to cdsarc.u-strasbg.fr.

Fig. 8. Geometry of the 22 June 2008 event on Earth. As predicted, it was actually a double occultation of the same star by Pluto and Charon. The shadow paths (central bold lines with Charon above, Pluto below) crossed South Australia, Namibia and La Reunion Island. The observations were attempted from many stations, indicated by star symbols, and eventually recorded from five sites in Australia and one site in La Reunion Island in the Indian Ocean. Dots mark 1 minute time intervals and indicate shadow speed. Apparent diameters of Charon (50 mas) and Pluto (100 mas) define their visibility path widths, outlined by the parallels to the central path.
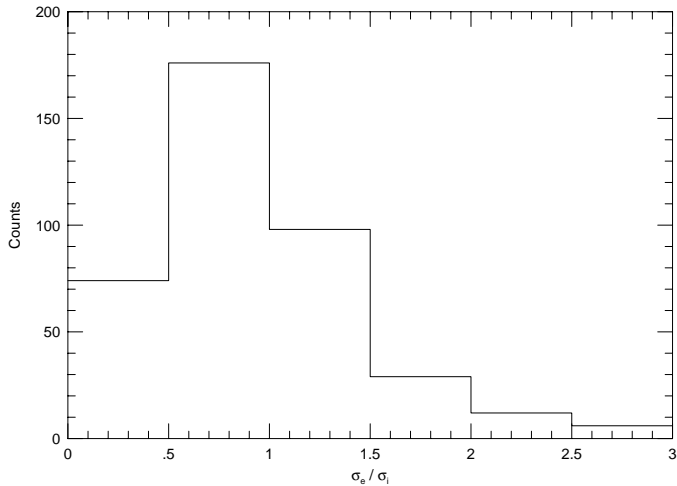
The astrometry of about 110GB of processed WFI images, first for Field Distortion Pattern (FDP) determination, then for the catalog, was made in automatic fashion with speed and precision by PRAIA - the Platform for Reduction of Astronomical Images Automatically (Assafin 2006).

One aspect of the work was deriving FDPs for all CCDs in the WFI mosaic. This allowed for the use of a simple linear model to relate measurements and sky-plane projected catalog reference positions, thus granting higher star/parameter ratios and robust astrometric results. Let σ_e be the external standard deviations of (Δx, Δy) offsets from the same bin, computed over distinct FDPs from different runs, and be σ_i the internal standard deviations computed over bins within the same FDP. Figure 9 plots the count distribution of σ_e / σ_i ratios computed for FDPs derived from September and October 2007, as well as from other telescope runs during 2007 and 2008, with detector maintenance in between. Since σ_i is of the order of UCAC2 position mean errors and since the distribution peaks at ratio = 0.75, we conclude that the derived FDPs are representative of the WFI distortions within at least about 50 mas, for any run made at the ESO2p2/WFI - even after WFI maintenance. This means that the derived FDPs may be promptly used for WFI astrometry at the 50mas level. The WFI FDP offsets obtained from September and October 2007 runs are available under request to the author. But, for better astrometric results, like in this work, dedicated FDP observations for each run are recommended, followed by the relatively simple astrometric procedures described in Sect. 4. In all, our method follows a different approach than that described in Anderson et al. (2006) and references therein for the astrometry of WFI mosaics.

Table 9. Sample from prediction tables for stellar occultations by Pluto.

d m year	h m s	RA (ICRS) Dec		C/A P/A	v D	R* J* H* K*	λ	LST	Δe_α	Δe_δ pm ct fg
		h m s	° ′ ″	mas °	km s^{-1} AU		°	h:m	mas	mas
22 06 2008	19 10 11	17 58 33.0155	-17 02 38.344	185 176.12	-23.80 30.47	12.9 11.7 11.6 11.4	071	23:53	+00.0	+74.5 ok uc 0
24 06 2008	10 36 55	17 58 22.3931	-17 02 49.335	168 355.86	-23.74 30.47	16.3 12.8 11.9 11.7	197	23:46	+00.0	+74.6 ok 2m 0
25 08 2008	04 34 51	17 53 27.1046	-17 15 27.526	169 328.87	-08.39 31.06	14.9 11.1 10.1 09.8	226	19:38	+00.0	+79.8 ok 2m 0

Prediction tables list event date and instant (UTC), the ICRS (J2000) star coordinates at occultation, the closest apparent distance between star and body (C/A), the position angle (P/A) of the shadow across the Earth (counter-clockwise, zero at South), the velocity in km s^{-1}, the distance (D) to the Earth (AU), longitude (λ) of the sub-solar point, local solar time (LST), (Δe_α, Δe_δ) ephemeris offset correction to the DE418 and plu017 ephemerides in (RA, DEC) for the central instant (see Sect. 6), catalog cross-identification (uc = UCAC2, 2m = 2MASS, fs = field star), proper motion existence and multiplicity flags (see Sect. 4.4), estimated star catalog position errors (E_α, E_δ) and proper motions (μ_α, μ_δ). R*, J*, H* and K* are star magnitudes normalized to a reference shadow velocity (v) of 20 km s^{-1}. The complete table set of 2008–2015 predictions for Pluto, Charon, Hydra and Nix is available in electronic form via anonymous ftp to cdsarc.u-strasbg.fr.

Fig. 9. Count distribution of σ_e/σ_e ratios. σ_e is the standard deviation of (Δx, Δy) offsets of the same bin computed over distinct FDPs from different runs. σ_i is computed over bins within the same FDP. As distribution peaks at 0.75, we conclude that FDPs are stable at least within 50 mas over distinct runs, independent of WFI maintenance.

Computation of new stellar proper motions using the 2MASS and USNO B1.0 as first epoch also enhanced the obtained catalog positions. For faint stars in particular, computing of proper motions instead of the direct use of USNO B1.0 own proper motions avoids the zero point issue warned by the authors (Monet et al. 2003). The computed proper motions not only bettered the predictions of upcoming events, but also improved the astrometric prediction and follow up feasibility of those events more distant in the future.

In all, the obtained astrometric catalog represented an improvement over predictions based on GSC2.3, USNO B1.0 or UCAC2 positions. In comparison, stars fainter than about R = 12 were better imaged with the ESO2p2/WFI (see Fig. 3 and Fig. 5). Also, as the sky path was covered by overlapping 30′ size CCD mosaics, we have overcome the problem of position zero-point errors inherent to predictions based on single catalog positions or originated from CCD observations with small FOV.

Note that we have not applied any UCAC2 to ICRS corrections to the derived catalog of star positions. Contrary to the UCAC2-based star positions derived from the astrometric LNA follow-up program between 2005-2008, which were used to compute ephemeris offsets (see Sect. 6), here we have preserved the original star positions obtained in the catalog. We give freedom to the user to decide what corrections should be applied, if any. Once a correction is established, it can be applied to the positions in the star catalog or, alternatively, can enter directly as a shift in the occultation shadow paths here predicted. UCAC2 to ICRS corrections can be computed from the comparison of optical versus VLBI positions of selected ICRF quasars nearby the sky path of Pluto along the years. The corrections described in Sect. 6 are only valid for UCAC2-based star positions around about 10 degrees from 2006.5 Pluto's coordinates, in which case they were $\Delta\alpha\cos\delta$ = -12 ±8 mas and $\Delta\delta$=−5 ±7 mas. Until 2015, Pluto will have moved by more than 15 degrees in the sky, so that new ICRF quasars need to be selected and new corrections evaluated. This issue will be addressed in future releases of the produced star catalog, including the possible use of future improved versions of the UCAC catalog itself (UCAC3, etc) as reference frame in the astrometry of the WFI mosaics.

A number of stellar occultations between 2005–2008 have been correctly predicted and successfully observed as predicted for stars between 13 < R < 16 (see Table 7), based on CCD observations made at LNA telescopes in Brazil. From these past occultations successfully recorded and fitted, a linear drift with time in declination for Pluto's ephemerides (DE418 and plu017) could be determined (see Table 8 and Fig. 6). This drift was taken into account to correctly describe the sky path of Pluto and its satellites and was an important step in our star candidate search.

On the other hand, no ephemeris correction was attempted for right ascension. Although an oscillation pattern related to an error in Pluto's heliocentric distance (geocentric parallax error) cannot be ruled out, none of the attempted models for this scenario could fit the more dispersed right ascension ephemeris offsets derived from the studied occultations, at least well below 50 mas (in the case of declination, a standard deviation of only 14.4 mas was achieved after the linear fitting). The issue deserves further investigation, but from a pragmatic point of view it is of

Table 11. Comparison between WFI-based and LNA-based old predictions.

| | LNA - WFI | | WFI stars | | |
| | $\Delta\alpha\cos\delta$ | $\Delta\delta$ | E_α | E_δ | Mag. |
Occultation	mas	mas	mas	mas	R
22 June 2008	−11	+03	40	15	12.9
24 June 2008	+14	−11	24	21	16.3
25 August 2008	−08	−15	58	13	14.9

Comparison between star positions from WFI-based (Table 9) and LNA-based (Table 7) past predictions for Pluto stellar occultations occurred in 2008. The position differences are in very good agreement, within the expected WFI-based star catalog position error estimates.

secondary importance to predictions, since right ascension ephemeris offsets do not affect the geographic latitude of the occultation shadow path over the Earth, and will only cause a marginal error in the predicted central instant of the event by just a few minutes at most, and even so only when far from opposition.

No threshold in R magnitude was established in the search for candidates. Pluto is crossing interestellar clouds, so relatively faint R objects may turn out to be bright infrared stars, perfect targets for the SOFIA observatory (Gehrz et al. 2009) and for ground-based instruments well equipped with H, J or K band detectors (H, J and K magnitudes are promptly available in the catalog if the star belongs to the 2MASS). Besides, events may be also favoured by slow shadow speeds of less than 20 km s^{-1}. Also, no constrains on geographic place where applied, as in principle SOFIA observations can be done from any sub-solar point on Earth. Even so, finding charts are also made available for events visible at regions well covered by instruments such as in North and South America, Europe, South Africa, Australia, Japan and Hawaii (see comment on web page reports below). Events in daylight at sub-planet point were not excluded either, as they could yet be observable in the dark, right above the horizon, from places near Earth terminator.

All through the paper, we did not distinguish between past and future predictions, publishing all found occultations for the sky path covered (or to be covered) by Pluto between 2008–2015. The importance of predictions for occultations still to come is obvious. But, the predictions of past occultations are also useful, for at least three reasons. First, they can be used by anyone as reference for ongoing fittings of light curves of recent past observed events. Second, they serve to derive ephemeris drifts by comparing expected and observed C/A and P/A values. Finally, they can be used as external check for the accuracy and precision of our WFI predictions.

In this way, we have compared star positions from WFI-based (Table 9) and LNA-based (Table 7) for three past, common predictions for Pluto stellar occultations occurred in 2008. The star position differences - and thus, the predictions - are in very good agreement within the expected WFI-based star catalog position error estimates. Table 11 displays this comparison.

In general, assuming a bulk error of 30 mas for C/A from the estimated errors of the WFI catalog star positions and from the errors of the derived ephemeris offsets, we can state that the shadow path uncertainties over Earth are of the order of less than 800 Km for the WFI occultation predictions.

Continuous observation of Pluto and candidate stars are recommended, and this effort is now facilitated by the produced catalog. Astrometric follow up is important in predictions due to the need for position refinements, and we hope that this task has been made easier now with the availability of the generated star catalog. Even astrometry with the use of modest FOV observations becomes feasible, as the zero-point error of our catalog is rather small and its magnitude completeness is about R = 18–19. Once new occultations are successfully recorded and analyzed, one can further improve the accuracy of Pluto's ephemeris offsets, allowing for a continuous fine tunning in the predictions. Besides, the photometric information contained in the catalog may be also useful in the observational preparation for the occultation itself.

We remark that updates on the ephemeris offsets or on candidate star positions can be easily taken into account for upgrading the geometric conditions of the predicted events. Updated reports and finding charts are made available in a continuous basis by the group at http://www.lesia.obspm.fr/perso/bruno-sicardy/.

We also emphasize the importance of predictions for stellar occultation by TNOs in general. Astrometry of candidate stars and determination of ephemeris offsets are utterly needed for these objects. Efforts are right now being made in this direction, by a similar observational program carried out by our group at the ESO2p2/WFI. Among other similar projects carried out by other active groups in the U.S.A., this effort comes together with a long term international campaign coordinated by the Observatoire de Paris for this purpose.

References

Acton, C.H. 1996, P&SS, 44, 65
Anderson, J., Bedin, L. R., Piotto, G., Yadav, R. S., Bellini, A. 2006, A&A, 454, 1029
Arias, E.F., Charlot, P., Feissel, M., Lestrade, J.-F. 1995, A&A, 303, 604
Assafin, M. 2006, Bol. Soc. Astron. Bras. 26(1), 189
Assafin, A., Nedelcu, D. A., Badescu, O., Popescu, P. , Andrei, A. H., Camargo, J. I. B., da Silva Neto, D. N., Vieira Martins, R. 2007, A&A, 476, 989
Assafin, M., Monken Gomes, P.T., da Silva Neto, D.N., Andrei, A.H., Vieira Martins, R., Camargo, J.I.B., Teixeira, R., Benevides-Soares, P. 2005, AJ, 129, 2907
Assafin, A., Vieira Martins, R., Andrei, A. H. 1997, AJ, 133, 1451
Brosch, N. 1995, MNRAS, 276, 571
Buie, M. et al. 2009, BAAS, 40, 4805
Cutri, R. M., et al. 2003, The 2MASS Point Source Catalog, University of Massachusetts, the Infrared Processing and Analysis Center(IPAC/Caltech), NOAO and the Smithsonian Institute
Elliot, J. L., et al. 1995, Nature, 373, 46
Elliot, J. L., Ates, A., Babcock, B. A., et al. 2003, Nature, 424, 165
Elliot, J. L., Person, M. J., Gulbis, A. A. S., et al. 2007, AJ., 134, 1
Feissel, M. & Mignard, F. 1998, A&A, 331, 33
Folkner, W. M., Standish, E. M., Williams, J. G., Boggs, D. H. 2007, Jet Propulsion Laboratory, California Institute of Technology, Memorandum IOM 343R-07-005

Gehrz, R. D., Becklin, E. E., de Pater, I., Lester, D. F., Roellig, T. L., Woodward, C. E. 2009, AdSpR, 44, 413

Gulbis, A. A. S., Elliot, J. L., Person, M. J., Adams, E. R., Babcock, B. A., Emilio, M., Gangestad, J. W., Kern, S. D., Kramer, E. A., Osip, D. J., Pasachoff, J. M., Souza, S. P., Tuvikene, T. 2006, Nature, 439, 48

Hansen, C. J. & Paige, D. A. 1996, Icarus, 120, 247

Jones, H., Valdes, F. 2000, "Handling ESO WFI Data With IRAF", ESO document number 2p2-MAN-ESO-22200-00002.

Lasker, B. M. et al. 2008, AJ, 136, 735

Lellouch, E., Sicardy, B., de Bergh, C., Käuf, H.-U., Kassi, S., Campargue, A. 2009, A&A, 495, L17

McDonald, S. W. & Elliot, J. L. 2000a, AJ, 119, 1999

McDonald, S. W. & Elliot, J. L. 2000b, AJ, 120, 1599

McKinnon, W. B., Simonelli, S. P., Schubert, G. 1997, in Pluto and Charon (eds Stern, S. A. & Tholen, D. J.) 295 (Univ. Arizona Press, Tucson)

Millis, R. L. et al. 1993, Icarus, 105, 282

Mink & Klemola 1985, AJ 90, 1894

Moffat, A.F.J. 1969, A&A, 3, 455

Monet, D., Levine, S. E., Canzian, B., et al. 2003, AJ, 125, 984

Olkin, C. et al. 2009, in preparation

Perryman, M. A. C. et al. 1997, A&A, 323, 49

Person, M. J., Elliot, J. L., Gulbis, A. A. S., Pasachoff, J. M., Babcock, B. A., Souza, S. P., Gangestad, J. 2006, AJ, 132, 1575

Sicardy, B., Widemann, T., Lellouch, E., et al. 2003, Nature, 424, 168

Sicardy, B. et al. 2006, Nature, 439, 52

Sicardy, B. et al. 2009, Monitoring Plutos atmospheric activity from stellar occultations: method and 2006-2007 campaign(in preparation)

Stansberry, J. A., Lunine, J. I., Hubbard, W. B., Yelle, R. V., Hunten, D. M. 1994, Icarus, 111, 503

Stone, R.C. 1989, AJ, 97, 1227

Tholen, D.J., Buie, M. W., Grundy, W. M., Elliott, J. L. 2008, AJ, 135, 777

Tody, D. 1993, "IRAF in the Nineties" in Astronomical Data Analysis Software and Systems II, A.S.P. Conference Ser., Vol 52, eds. R. J. Hanisch, R. J. V. Brissenden and J. Barnes, 173.

Valdes, F.G. 1998, "The IRAF Mosaic Data Reduction Package" in Astronomical Data Analysis Software and Systems VII, A.S.P. Conference Ser., Vol 145, eds. R. Albrecht, R. N. Hook and H.A. Bushouse, 53

Vieira Martins, R. et al. 2009, PSF astrometry. Precise Pluto positions from unresolved Pluto/Charon images (in preparation)

Walker, A. R. 1980, MNRAS, 192, 47

Yelle, R. V. & Elliot, J. L. 1997, in Pluto and Charon (eds Stern, S. A. & Tholen, D. J.) 347 (Univ. Arizona Press, Tucson)

Yelle, R. V. & Lunine, J. I. 1989, Nature, 239, 288

Young, E. F., French, R. G., Young, L. A., et al. 2008, AJ., 136, 1757

Young, L. et al. 2007, BAAS, 39, 6204

Zacharias, N., Urban, S.E., Zacharias, M. I., Wycoff, G. L., Hall, D. M., Monet, D. G., Rafferty, T. J. 2004, AJ, 127, 3043